Spectral Properties of Selected Superconducting Materials

L. S. Fletcher,* G. P. Peterson,† and R. K. Pandey‡
Texas A&M University, College Station, Texas 77843
and
G. R. Cunnington§
Lockheed Research and Development, Palo Alto, California 94304

Introduction

DURING the 1960s, low-temperature superconducting materials were developed for specialized applications such as ultrasensitive magnetic field detectors. With the development of high-temperature superconductors, other applications not previously feasible have become much more attractive. These applications include electronic switching devices and the use of superconductors for radiation shielding. Because of the so-called "Meisner effect" in which magnetic fields are excluded, high-temperature superconducting materials may be suitable for aerospace applications requiring very low-emittance or switchable-emittance properties. Low-emittance applications include enhanced thermal isolation required for cryogenic devices and systems, whereas switchable properties are desirable for variable conductance devices and for optical signature control. As a consequence, high-temperature superconducting materials could be used as thin films to minimize weight and provide the rapid transient response so important in the application of switchable properties.

Although there have been numerous investigations of low-temperature superconducting materials,[1] only limited data have been found for the thermophysical properties of the more recently developed high-temperature superconductors. There have been several investigations involving selected properties of high-temperature superconductors[2-5] including both thermal and electrical properties. However, the radiation properties of these materials have generally not been included in the reported literature. Tajima et al.[6] reported some spectral reflectance data for compounds of

$YBa_2Cu_3O_7$
La_2CuO_4
$(La_{1-x}Sr_x)_z\ CuO_4$

One important question is as yet unanswered: "Can very high reflectance be achieved using high-temperature superconductors or are they limited by the anisotropic nature of the materials and the relatively low carrier concentrations found in oxide superconductors?" Because most of the available data deal with the longitudinal properties rather than the transverse properties, solutions for two-dimensional electromagnetic problems are not well understood.

In an attempt to resolve this question, an investigation was undertaken to experimentally determine the radiative properties of selected high-temperature superconducting materials.

Presented as Paper 89-1674 at the AIAA Thermophysics Conference in Buffalo, NY, June 12–14, 1989; received June 16, 1989; revision received Sept. 21, 1989.

*Thomas A. Dietz Professor of Mechanical Engineering. Fellow AIAA.

†Associate Professor of Mechanical Engineering. Senior Member AIAA.

‡Professor of Electrical Engineering.

§Senior Member Research Laboratory. Associate Fellow AIAA.

Table 1 Superconducting Material Properties[a]

Property	Hot pressed	Cold pressed
Density, g/cm^3	5.0±0.005 at 300 K	3.72–3.76 at 300 K
T_c	94 K	91.7 K
Mechanical bonding	Very good	Poor

[a]$YBa_2Cu_3O_7$ hot pressed and cold pressed.

Experimental Program

Two basic techniques exist for preparing high-temperature superconductors.[7] These include either hot or cold pressing. Generally, cold-pressed materials result in lower densities, often 50–60% below the theoretical values. These materials are prone to surface damage by water, air, and acids. Hot-pressed materials, on the other hand, provide a high-quality, single-phase ceramic sample of orthorhombic structure. In addition, the hot-pressed samples provide a well-defined superconducting phase transition at 94 K, improved reproducibility at elevated levels of excitation, and an increased ability to withstand thermal cycling. This investigation involved the use of both hot-pressed and cold-pressed YBaCuO samples.

The 1-2-3 YBaCuO materials were prepared by thoroughly mixing the ingredients in a ball mill. The mixture was then reacted in air at 1198 K in a clean high-purity-grade alumina crucible. The solid lump material formed after reaction was ground to a fine powder and rereacted at 1248 K in an oxygen atmosphere for several subsequent heating and cooling cycles to drive off the remaining carbon dioxide. At this point, the resulting material was suitable for processing into dense polycrystalline samples, for epitaxial deposition as a superconducting film on an appropriate substrate or for the growth of bulk single crystals. For this investigation, the material was pressed to a maximum value of 69 MPa, while the temperature was raised to a maximum value of 923 K. The resulting samples were then sintered and annealed, resulting in a sample which had optically smooth surfaces but was not transparent. Details of this technique have been reported by Pandey et al.[7] and selected material properties are provided in Table 1.

The radiation properties of superconducting materials were characterized by measuring the spectral normal emittance over a wavelength range of 6–30 μm at selected temperatures. The physical arrangement of the test facility used for these measurements is shown in Fig. 1. A 1-cm^2 sample, 2–3 mm thick, was mounted on a temperature-controlled sample block connected by a thermolink to a cryogenically cooled cold block. An electrical heater was incorporated into the thermolink to permit accurate control of the sample temperature. A blackbody and a polished gold sample were placed on the sample block adjacent to the test sample. The spectrometer alternatively viewed the gold sample, the blackbody, and the test sample.

A liquid-nitrogen-cooled enclosure surrounded the test assembly and prevented ambient radiation from being reflected from the sample into the field of view of the spectrometer. The gold sample provided a contamination monitor as well as a measure of any reflected extraneous energy from the

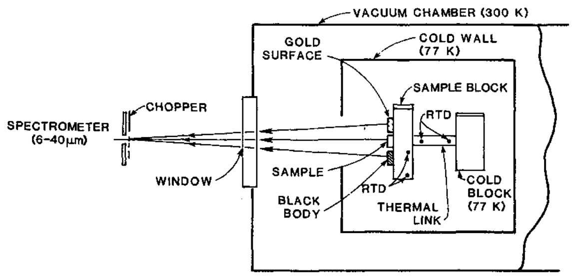

Fig. 1 Spectral-emittance apparatus.

surroundings, including the vacuum chamber window, and it was used to verify the ambient shielding efficiency. The blackbody provided a calibration reference at the test sample temperature. The blackbody used in this investigation was a 5-mm diam by 25-mm deep, vee-bottomed cavity coated with "Red Spot" flat black paint. Cavity emittance was calculated to be greater than 0.97 for a wavelength of 26 μm which was the limitation of the spectral reflectance data. The gold sample was of highly specular nature and had a total hemispherical emittance of 0.014 at 80 K, as noted by Cunnington et al.[8]

The sample assembly was placed in a vacuum chamber having a turbomolecular pumping system with a liquid-nitrogen cold shroud. The chamber was maintained at a pressure of less than 10^{-4} Pa. A cesium-iodide window was located in one end of the vacuum chamber to permit viewing of the test specimen and the gold and blackbody reference sources with the spectrometer. The spectrometer had both Ge:Zn and vacuum thermocouple detectors with a wavelength measurement range of 10-40 μm.

In addition to the spectral-emittance measurements, spectral-reflectance measurements were made on the test specimens. A Cary Model 17 Spectrometer with integrating sphere attachment and a Gier-Dunkle Model HC300 heated cavity reflectometer were used to measure the near-normal spectral reflectance of the specimens at 298 K. Near-normal spectral-reflectance measurements were also made at 80-85 K for wavelengths of 0.64 μm and 10.6 μm using helium-neon and carbon dioxide lasers with silicon and Hg:Cd:Te detectors. These measurements were made with the specimens mounted in the same manner as for the spectral-emittance measurements.

Results and Discussion

Spectral-reflectance measurements were performed initially at 298 K for the samples of the $YBa_2Cu_3O_7$ material. These measurements were made over the wavelength range of 0.27-26 μm. Spectral-reflectance measurements were then made at 80-85 K at wavelengths of 0.63 μm and 10.6 μm using unpolarized laser sources. These data are shown in Fig. 2 and compared with data provided by Tajima et al.[6] for the same type of material. A small increase in normal spectral reflectance was observed at 10.6 μm by reducing the sample temperature below the critical temperature of 94 K. Although these results do not show a change in reflectance consistent with the change in electrical resistivity, the frequency corresponding to a wavelength of 10.6 μm may not be appropriate for the energy gap of the material. The lower reflectance of the cold-pressed material with respect to the hot-pressed sample of 298 K is consistent with its higher electrical resistivity.

Because the hot-pressed specimen cracked during the second reflectance measurement cooling cycle, the primary emittance measurements were carried out on the cold-pressed specimen. The cracking was most likely due to the highly crystalline anisotropy of the sample. The spectral normal emittance data for the cold-pressed sample are shown in Fig. 3 for three different

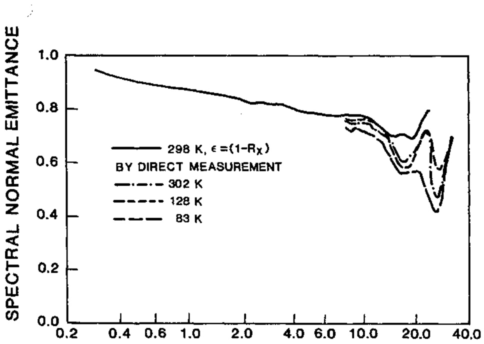

Fig. 2 Near-normal spectral reflectance for hot-pressed and cold-pressed $YBa_2Cu_3O_7$.

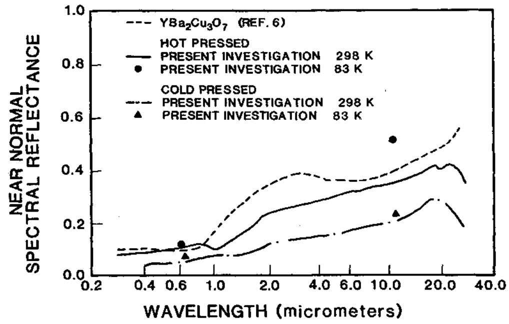

Fig. 3 Spectral normal emittance of cold-pressed $YBa_2Cu_3O_7$.

temperatures. These data indicate that the emittance does not change significantly with decreasing temperature, even in the superconducting region. The accuracy of these data are calculated to be 0.04 in absolute emittance from 10-25 μm and 0.07 from 25-40 μm. The very small temperature dependence of spectral emittance indicates that the material behaves more like a semiconductor or insulator rather than a normal conductor.

Several possible reasons for the strong departure in the emittance data from that which would be expected considering electrical resistivity data have been examined. First, the material may be an anisotropic conductor, that is, electron motion may be unidirectional, and thus the energy gap may be very broad, 3-5 eV or greater. This would negate any optical benefit in the wavelength region measured for this paper. Second, electron-phonon interactions may preclude a three-dimensional uniform field within the material. Third, the manufacturing processes and/or subsequent handling for the measurements may not be consistent with optimizing material properties. Handling and mounting may have induced lattice strains, but such an occurrence is believed to be a remote possibility. The optical properties behave more like a semiconductor having a carrier concentration of 10^{20}-10^{21} cm^{-3}.

Conclusions

Near-normal spectral-reflectance measurements were made for wavelengths of 0.27-26 μm at a temperature of 298 K with additional data obtained at 83 K for two wavelengths. Spectral normal emittance values were obtained for cold-pressed material over a wavelength range of 10-38 μm for temperatures of 84, 128, and 302 K.

The data indicate that the cold-pressed material exhibited a lower reflectance with respect to the hot-pressed sample at the same temperature, consistent with its higher electrical resistivity. The emittance data do not change significantly with temperature, suggesting that the material behaves more like an insulator or semiconductor rather than a normal conductor.

A more interesting measurement would be that of total hemispherical emittance of the materials as a function of temperature in the temperature range of 40-80 K. Since a major fraction of the radiated energy occurs at wavelengths greater than 50 μm, these data would be a better test of the large band-gap model.

References

[1]Schmidt, C., "Simple Method to Measure the Thermal Conductivity of Technical Superconductors, e.g., NbTi," *Review of Scientific Instruments*, Vol. 50, No. 4, 1979, pp. 454-457.

[2]Freeman, J. J., Friedman, T. A., Ginsberg, D. M., Chen, J., and Zangvil, A., "Low-Temperature Thermal Conductivity of $YBa_2Cu_3O_{7-s}$," *Physical Review B*, Vol. 36, No. 16, 1987, pp. 8786-8787.

[3]Morelli, D. T., Heremans, J., and Swets, D. E., "Thermal Conductivity of Superconductive Y-Ba-Cu-O," *Physical Review B*, Vol. 36, No. 7, 1987, pp. 3917-3919.

[4]Collocott, S. J., White, G. K., Dou, S. X., and Williams, R. K., "Thermal Properties of the High Tc Superconductors $La_{1.85}Sr_{0.15}$-

CuO_4 and $YBa_2Cu_3O_7$," *Physical Review B*, Vol. 36, No. 10, 1987, pp. 5634-5685.
[5]Heremans, J., Morelli, D. T., Smith, G. W., and Strite, III, S. C., "Thermal and Electronic Properties of Rare-Earth Ba_2Cu_3Ox Superconductors," *Physical Review B*, Vol. 37, No. 4, 1988, pp. 1604-1610.
[6]Tajima, S., Uchida, S., Tanaka, S., Kanbe, S., Kitazawa, K., and Fueki, K., "Plasma Spectra of New Superconductors $(La_{1-x}A_x)_2$-CuO_4," *Japanese Journal Applied Physics*, Vol. 26, 1987, pp. L432-L433.
[7]Pandey, R. K., Gilbert, G. R., Kirk, W. R., Kobiela, P. S., Clearfield, A., and Squattrito, P. J., "Processing of Single-Phase Ceramic 1-2-3 YBaCu-Oxide Superconductor by Hot Pressing," *Journal of Superconductivity*, Vol. 1, No. 1, 1988, pp. 45-52.
[8]Cunnington, G. R., Bell, G. A., Armaly, B. F., and Tien, C. L., "Total Emittance Measurements of Thin Metallic Films at Cryogenic Temperatures," *Journal of Spacecraft and Rockets*, Vol. 7, No. 12, 1970, pp. 1496-1499.

View Factor Between Differing-Diameter, Coaxial Disks Blocked by a Coaxial Cylinder

D. E. Bornside* and R. A. Brown†
Massachusetts Institute of Technology, Cambridge, Massachusetts 02139

Introduction

VIEW-factor algebra can be used to derive the view factors for complicated geometries from available view factors for simpler geometries.[1-3] This approach is particularly useful for the numerical analysis of heat-transfer problems involving diffuse-gray radiative interchange among the surfaces of the system, where finite-element and finite-difference methods require calculation of the view factors between the many surfaces which correspond to the numerical grid.

Radiative heat transfer is extremely important in Czochralski crystal growth of semiconductor materials.[4] Here a cylindrical crystal is grown from its melt by withdrawing the crystal and adjusting the heat transfer needed for solidification. When the radiative transfer is diffuse and gray and the crystal is a perfect cylinder, the necessary view factors can be derived using view-factor algebra in conjunction with view factors for three simple geometries available in the literature.[5] The computational effort is reduced if these view factors are available as algebraic expressions and are not evaluated numerically.

One particular view factor needed for the Czochralski configuration is that between parallel, coaxial disks of different diameters that are separated by a solid, coaxial cylinder (see Fig. 1). Minning[6] and Holchendler and Laverty[7] both attempted to derive this view factor. (Holchendler and Laverty's analysis is for a frustrum, which is a cylinder in the limit when the diameters at its two ends are equal, separating the two opposing disks.) They both succeeded in deriving the view factor from a differential surface to an opposing finite disk. However, neither was able to integrate this expression to obtain a closed-form result for the view factor from a finite disk to an opposing finite disk because of the complexity of the resulting integrand. In this Note, a closed-form expression for this view factor is presented that is valid when the disks both have finite radius.

Analysis

The expression presented by both Minning[6] and Holchend- ler and Laverty[7] for the view factor from a differential surface to an opposing finite disk is derived using the contour integral method[8]:

$$F_{dA_\rho-A_a}=\frac{\cos^{-1}\frac{c}{a}}{2\pi}-\frac{c^2-\rho^2-h^2}{\pi\sqrt{(c^2+\rho^2+h^2)^2-4\rho^2c^2}}\tan^{-1}\left[\sqrt{\frac{(c^2+\rho^2+h^2+2\rho c)(\rho-c)}{(c^2+\rho^2+h^2-2\rho c)(\rho+c)}}\right]+\frac{a^2-\rho^2-h^2}{\pi\sqrt{(a^2+\rho^2+h^2)^2-4\rho^2a^2}}$$
$$\times\tan^{-1}\left[\sqrt{\frac{(a^2+\rho^2+h^2+2a\rho)(\rho a-c^2+\sqrt{\rho^2-c^2}\sqrt{a^2-c^2})}{(a^2+\rho^2+h^2-2a\rho)(\rho a+c^2-\sqrt{\rho^2-c^2}\sqrt{a^2-c^2})}}\right] \tag{1}$$

Here a is the radius of the finite disk, c is the radius of the solid cylinder, h is the height of the cylinder, which is also the axial distance between the finite disk and the plane defined by the differential surface, and ρ is the distance between the differential surface and the vertical axis. The view factor $F_{dA_\rho-A_a}$ is from the differential surface with area dA_ρ to the finite disk with outer radius a, inner radius c, and area A_a. Equation (1) is equivalent to Eq. (6) in Minning's paper and to Eq. (13) in Holchendler and Laverty's paper. There are some sign mistakes in Eq. (6) in Minning's paper.

The view factor from a finite disk with outer radius b and inner radius c to a disk with outer radius a and inner radius c is obtained by integrating Eq. (1) as

$$A_bF_{A_b-A_a}=2\pi\int_c^b F_{dA_\rho-A_a}\rho d\rho \tag{2}$$

where $F_{A_b-A_a}$ is the view factor from a disk with outer radius b, inner radius c, and area A_b to a coaxial, parallel disk with outer radius a, inner radius c, and area A_a. The disks are separated by a solid, coaxial cylinder of radius c and height h. Substituting

Received July 17, 1989; revision received Oct. 2, 1989.
*Postdoctoral Research Associate, Department of Chemical Engineering and Materials Processing Center.
†Professor and Head, Department of Chemical Engineering and Materials Processing Center.